www.sciencemag.org/cgi/content/full/1179052/DC1

Supporting Online Material for

Detection of an Infectious Retrovirus, XMRV, in Blood Cells of Patients with Chronic Fatigue Syndrome

Vincent C. Lombardi, Francis W. Ruscetti, Jaydip Das Gupta, Max A. Pfost, Kathryn S. Hagen, Daniel L. Peterson, Sandra K. Ruscetti, Rachel K. Bagni, Cari Petrow-Sadowski, Bert Gold, Michael Dean, Robert H. Silverman, Judy A. Mikovits*

*To whom correspondence should be addressed. E-mail: judym@wpinstitute.org

Published 8 October 2009 on *Science* Express
DOI: 10.1126/science.1179052

This PDF file includes:

Detection of an Infectious Retrovirus, XMRV, in Blood Cells of Patients with Chronic Fatigue Syndrome

Vincent C Lombardi, Francis W Ruscetti, Jaydip Das Gupta, Max A Pfost, Kathryn S Hagen, Daniel L Peterson, Sandra K Ruscetti, Rachel K Bagni, Cari Petrow-Sadowski, Bert Gold, Michael Dean, Robert H Silverman, Judy A Mikovits*

Supporting Online Material

* E-mail: judym@wpinstitute.org, Telephone: 775-224-3892, Fax: 775-996-7159.

This PDF contains:

Supporting Online Materials and Methods

Patient samples. Banked samples were selected for this study from patients fulfilling the 1994 CDC Fukuda Criteria for Chronic Fatigue Syndrome (S1) and the 2003 Canadian Consensus Criteria for Chronic Fatigue Syndrome/myalgic encephalomyelitis (CFS/ME) and presenting with severe disability. Samples were selected from several regions of the United States where outbreaks of CFS had been documented (S2). These are patients that have been seen in private medical practices, and their diagnosis of CFS is based upon prolonged disabling fatigue and the presence of cognitive deficits and reproducible immunological abnormalities. These included but were not limited to perturbations of the 2-5A synthetase/RNase L antiviral pathway, low natural killer cell cytotoxicity (as measured by standard diagnostic assays), and elevated cytokines particularly interleukin-6 and interleukin-8. In addition to these immunological abnormalities, the patients characteristically demonstrated impaired exercise performance with extremely low VO2 max measured on stress testing. The patients had been seen over a prolonged period of time and multiple longitudinal observations of the clinical and laboratory abnormalities had been documented.

DNA and RNA isolation. Whole blood was drawn from subjects by venipuncture using standardized phlebotomy procedures into 8-mL green-capped Vacutainers containing the anti-coagulant sodium heparin (Becton Dickinson, Franklin Lakes, NJ). Plasma was collected by centrifugation, aspirated and stored at -80 ºC for later use. The plasma was replaced with PBS and the blood resuspended and further diluted with an equal volume of PBS. PBMC were isolated by layering the diluted blood onto Ficoll-Paque PLUS (GE Healthcare, Waukesha, WI), centrifuging for 22 min at 800 g, aspirating the PBMC layer and washing it once in PBS. The PBMC (approximately 2 x 10^7 cells) were centrifuged at 500x g for 7 min and either stored as unactivated cells in 90% FBS and 10% DMSO at -80 ºC for further culture and analysis or resuspended in TRIzol (Invitrogen, Carlsbad, CA) and stored at -80 ºC for DNA and RNA extraction and analysis. DNA was isolated from TRIzol preps according the to manufacturer's protocol and also isolated from frozen PBMC pellets using the QIAamp DNA Mini purification kit (QIAGEN, Valencia, CA) according to the manufacturer's protocol, and the final DNA was resuspended in RNase/DNase-free water and quantified using the Quant-iT *Pico* Green dsDNA Kit (Invitrogen, Carlsbad, CA). RNA was isolated from TRIzol preps according to the manufacturer's protocol and quantified using the Quant-iT *Ribo* Green RNA kit (Invitrogen, Carlsbad, CA). cDNA was made from RNA using the iScript Select cDNA synthesis kit (Bio-Rad, Hercules, CA) according to the manufacturer's protocol.

PCR. To avoid potential problems with laboratory DNA contamination, nested PCR was performed with separate reagents in a separate laboratory room designated to be free of high copy amplicon or plasmid DNA. Negative controls in the absence of added DNA were included in every experiment. Identification

of XMRV *gag* and *env* genes was performed by PCR in separate reactions. Reactions were performed as follows: 100 to 250 ng DNA, 2 µL of 25 mM $MgCl_2$, 25 µL of HotStart-IT FideliTaq Master Mix (USB Corporation, Cleveland, OH), 0.75 µL of each of 20 µM forward and reverse oligonucleotide primers in reaction volumes of 50 µL. For identification of *gag*, 419F (5'-ATCAGTTAACCTACCCGAGTCGGAC-3') and 1154R (5'-GCCGCCTCTTCTTCATTGTTCTC-3') were used as forward and reverse primers. For *env*, 5922F (5'- GCTAATGCTACCTCCCTCCTGG-3') and 6273R (5'-GGAGCCCACTGAGGAATCAAAACAGG-3') were used. For both *gag* and *env* PCR, 94°C for 4 min initial denaturation was performed for every reaction followed by 94°C for 30 seconds, 57°C for 30 seconds and 72°C for 1 minute. The cycle was repeated 45 times followed by final extension at 72°C for 2 minutes. Six microliters of each reaction product was loaded onto 2% agarose gels in TBE buffer with 1 kb+ DNA ladder (Invitrogen, Carlsbad, CA) as markers. PCR products were purified using Wizard SV Gel and PCR Clean-Up kit (Promega, Madison, WI) and sequenced.

PCR amplification for sequencing full-length XMRV genomes was performed on DNA amplified by nested or semi-nested PCR from overlapping regions from PBMC DNA. For 5' end amplification of R-U5 region, 4F (5'-CCAGTCATCCGATAGACTGAGTCGC-3') and 1154R was used for first round and 4F and 770R (5'-TACCATCCTGAGGCCATCCTACATTG-3') was used for second round. For regions including *gag-pro* and partial *pol*, 350F(5'-GAGTTCGTATTCCCGGCCGCAGC-3') and 5135R (5'-CCTGCGGCATTCCAAATCTCG-3') was used for first round followed by second round with 419F and 4789R (5'-GGGTGAGTCTGTGTAGGGAGTCTAA-3'). For regions including partial *pol* and *env* region, 4166F (5'-CAAGAAGGACAACGGAGAGCTGGAG-3') and 7622R (5'-GGCCTGCACTACCGAAAT TCTGTC-3') were used for first round followed by 4672F (5'GAGCCACCTACAATCAGACAAAAGGAT-3') and 7590R (5'-CTGGACCAAGCGGTTGAGAATACAG-3') for second round. For the 3' end including the U3-R region, 7472F (5'-TCAGGACAAGGGTGGTTTGAG-3') and 8182R (5'-CAAACAGCAAAAGGCTTTATTGG-3') were used for first round followed by 7472F and 8147R (5'-CCGGGCGACTCAGTCTATC-3') for second round. The reaction mixtures and conditions were as described above except for the following: For larger fragments, the final extension was done at 68°C for 10 min instead of 72°C for 2 min. All second round PCR products were column purified as described above and overlapping sequences were determined with internal primers.

Nested RT-PCR for *gag* sequences was done as described (5) with modifications. GAG-O-R primer was used for 1st strand synthesis; cycle conditions were 52^{o}C annealing, for 35 cycles. For second round PCR, annealing was at 54^{o}C for 35 cycles.

PCR analysis performed on 20 of the identical patient PBMC DNA specimens stored at the NCI (Frederick, MD) since 2007 confirmed nearly identical *gag* sequences, thereby diminishing the possibility of laboratory contamination as a source of XMRV.

Phylogenetic Analysis. Sequences were aligned using ClustalX (S3). Clustal alignments were imported into MEGA4 to generate neighbor-joining trees using the Kimura 2-parameter plus Γ distribution (K80+Γ) distance model (S4). Free parameters were reduced to the K80 model, and α values were estimated from the data set using a maximum likelihood approach in PAUP*4.0 (Sinauer Associates, Inc. Publishers, Sunderland, MA, USA). The bootstrap consensus tree inferred from 1000 replicates is taken to represent the evolutionary history of the taxa analyzed. Accession numbers were acquired from GenBank. (http://www.ncbi.nlm.nih.gov/Genbank): FLV (NC_001940), MoMLV (NC_001501), XMRV VP35 (DQ241301), XMRV VP42 (DQ241302) XMRV VP62 (EF185282). Genomic Nonecotropic MLV Provirus Sequences were downloaded from PLOS Genetics (S5).

Isolation, separation and culture of primary cells. Leukopaks of peripheral blood from healthy donors were collected according to a NIH approved IRB #99-CC-0168 protocol. Patients' peripheral blood and plasma samples were from frozen banked samples obtained under NIH exempt status. Mononuclear leukocytes from both normal and patients' cells were isolated by Ficoll-Hypaque gradient centrifugation. The light density fraction (buffy coat) was collected and washed twice with PBS. PBMC were activated by 1 μg/mL PHA (Abbott Diagnostics, Abbott Park, IL) and after 72 hours the cells were cultured with 20 units/mL of IL-2 (Zeptometrix, Buffalo, NY) and subcultured every 3-5 days. For isolation of CD4+T cells, CD8, CD11b, CD14, CD19, CD33 and CD56 positive cells were removed using magnetic activated cell sorting (MACs) methods according to the manufacturer's instructions (Miltenyi Biotec, Inc., Auburn, CA). After isolation, the CD3+, CD4+ T cells (>95% pure) were cultured in RPMI-1640 medium supplemented with 10% fetal calf serum (FCS), 2 mM glutamine, 1 mM sodium pyruvate and antibiotics. $CD4^+$ T cells were activated by culturing with 20 units/mL of IL-2 and 1 μg/mL PHA.

In vitro expansion of primary B-cells. NIH 3T3 cells transduced with a retroviral vector expressing CD40L (gift of Eugene Barsov, NCI-Frederick) were maintained in Dulbecco's Modified Eagle's Medium (DMEM) (Invitrogen, Carlsbad, CA) supplemented with 10% calf serum (CS) (Lonza, Basel, Switzerland) and 1% penicillin, streptomycin and L-glutamine (Invitrogen, Carlsbad, CA) at 37°C with 5% CO_2. To stimulate B cell expansion, ~3.5 x 10^6 NIH3T3-CD40L cells were trypsinized (0.25% trypsin with EDTA)(Invitrogen, Carlsbad, CA), resuspended in 3 mL medium and irradiated with an absorbed radiation dose (rad) of 9600 using a $Cesium^{137}$ irradiator. Cells plus 7 mL medium were added to a T25 cell culture flask (Corning, Corning, NY) and allowed to adhere (2-3 h) to the flask surface (optimal density ~50%).

CD19+ B cells were isolated from PBMC using immunomagnetic bead technology (Miltenyi Biotec, Auburn, CA). CD19+ cells were separated from 10^8 freshly isolated PBMC by positive selection according to the manufacturer's protocol. After magnetic separation, CD19+ B cells (>95% pure) were added to

an irradiated NIH3T3-CD40L monolayer and incubated at 37 °C with 5% CO_2. Cultures were monitored for B cell proliferation and split 1:5 every 72-96 hr onto freshly irradiated NIH 3T3-CD40L monolayer. CD19+ primary B cells were cultured and expanded in primary B cell expansion media: Iscove's Modified Dulbecco's Medium (IMDM) (Invitrogen, Carlsbad, CA) + 10% FCS (Atlanta Biologicals, Lawrenceville, GA), 1% penicillin, streptomycin and L-glutamine (Invitrogen, Carlsbad, CA), 40 ng/mL interleukin 4 (IL-4) (PeproTech, Inc., Rocky Hill, NJ), 50 µg/mL holo-transferrin (Sigma, St. Louis, MO) and 5 µg/mL insulin (Invitrogen, Carlsbad, CA).

Cell culture and reagents. Raji, SupT1 and LNCaP were obtained from American Type Culture Collection (ATCC, Manassas, VA). The cells were maintained in RPMI-1640 supplemented with L-glutamine (2 mM), penicillin (100 U/mL), streptomycin (100 ng/mL), and FCS (10%) and subcultured 1:5 every 4-5 days. HCD-57 cells are a mouse erythroleukemia cell line that expresses both ecotropic and polytropic MLVs; HCD-57/SFFV are HCD-57 cells infected with SFFV. BaF3-ER cells are a murine pro B cell line engineered to express the erythropoietin receptor. BaF3ER-SFFV Env cells were derived and maintained as described (S6).

Flow cytometry for viral proteins. Adherent cells were incubated in trypsin for 10 minutes at 37^{o}C. After additional washes, adherent and suspension cells were incubated for 15 min at RT in 1 mL of paraformaldehyde (4% w/v in PBS), washed in permeabilization wash buffer (0.5% saponin 0.1%, sodium azide, 2% human AB sera in PBS) (PWB), and resuspended in 300 µL of permeabilization buffer (PBS with 2.5% saponin) (PB). After incubating at 22^{o}C for 20 min, 5 mL of human AB sera and either rat anti-MLV p30 mAb, rat anti-SFFV Env mAb, goat anti-Rauscher MLV gp70 Env, p30 Gag, or p10 Gag, or the appropriate isotype control (anti-rat IgG, rat myeloma supernatant, or preimmune goat serum) were added, and the cells incubated at 4^{o}C for an additional 30 min. Cells were then washed in PWB, resuspended in 100 µL of PB with 3 µL (0.6 µg) of FITC-conjugated goat anti-rat IgG or rabbit anti-goat antibody (BD PharMingen, San Jose, CA) and incubated for 20 min at 4^{o}C. The efficiency of permeabilization was determined using a FITC-conjugated anti-actin antibody. Cells were then washed twice in PB, resuspended in 500 µL of sheath fluid (BD PharMingen, San Jose, CA) to prevent clumping and analyzed by flow cytometry. For experiments in which purified cell populations were examined, cells were stained with an anti-CD3 or anti-CD19 antibody prior to permeabilization, and analyzed by gating on the $CD3^{+}$ or CD19+ subsets.

Western Blot (WB) analysis. Cells were pelleted, washed twice with PBS, and lysed for 30 min on ice in RIPA lysis buffer (50 mM Tris, pH 7.4, 150 mM NaCl, 0.25% deoxycholate,1% NP-40, and protease inhibitor cocktail (Sigma, St. Louis, MO). Debris was removed by centrifugation for 15 min at 21,000x g at 4^{o}C. Protein concentration was determined with the Bio-Rad Protein Assay reagent

and equal amounts of protein (70–200 ug) were separated by SDS-PAGE electrophoresis on 4-20% Tris-Glycine gels (Invitrogen, Carlsbad, CA) and then transferred to Immobilon-P membranes (Millipore, Billerica, MA). The membranes were blocked with 5% non-fat dry milk/1x TBST (Tris-buffered saline with 0.1% Triton X-100) for 1 h at room temperature, hybridized with the appropriate antiserum diluted in 5% non-fat dry milk/1xTBST for 2 h at room temperature or overnight at 4^{o}C, washed twice with 1xTBST, hybridized with the appropriate horseradish-peroxidase conjugated antibody diluted 1:5000 for 1 h at room temperature, and washed three times with 1xTBST. Hybridized bands were visualized using HyGlo chemiluminescent HRP antibody detection reagent (Denville Scientific, Metuchen, NJ) and exposed to film (Kodak, Rochester, NY). Antibodies used were a rat monoclonal Ab to SFFV gp55 Env (7C10), diluted 1:100 and detected with peroxidase-labeled anti-rat secondary antibody (Amersham, Waukesha, WI); goat anti-Rauscher MLV gp70 Env, p30 Gag and p10 Gag (provided by NCI); and goat anti-NZB xenotropic MLV (provided by NCI), all diluted 1:2500 and detected with peroxidase labeled anti-goat secondary antibody (Santa Cruz Biotechnology, Santa Cruz, CA).

Viral transmission. Frozen cell-free plasma and 0.22 µm filtered cell free supernatants from PBMC and T cell cultures were diluted 1:1 with tissue culture media and 600 µL aliquots were added to a six-well culture plate with the LNCaP cell line (50% confluent) or a million primary activated CD4+ T cells isolated from healthy donors. The plates were centrifuged for 5 min at 1500 RPM, rotated 180^{o} and centrifuged again for 5 min. The entire cycle was repeated once and cells were then diluted in their growth media. For cell-cell transmission, 1 x 10^{6} T cells or PBMC without any IL-2 in the growth media were added to a six-well culture plate with the LNCaP cell line (50% confluent) in 1 mL of media for 3 h. After 1 hr, T cells in suspension were removed and the LNCaP cells were grown for several passages in the absence of IL-2 which caused any remaining T cells to die. At the times after transmission indicated, protein analysis was done by western blot and flow cytometry.

Genotyping. The rs486907 R462Q SNP was genotyped using Applied Biosystems' Taqman® 5' nucleotidase assays, Taqman® Universal PCR Master Mix: No AmpErase UNG, and 5 ng of genomic DNA. The thermal cycling conditions consisted of an initial hold at 95^{o} C for 10 minutes followed by 50 cycles of a 15 second 95^{o} C denaturation step and a one minute 60^{o} C annealing and extension step. A 7900HT instrument was used to detect fluorescent probes, and Sequence Detection Software (SDS) v2.2 was used to discriminate alleles and call genotypes (Applied Biosystems, Foster City, CA). The variant is in Hardy-Weinberg equilibrium in both cases and controls. A Chi square test was performed for both genotypes and alleles of RNASEL comparing XMRV negative and XMRV positive controls. Both tests were not significant and the allele test is displayed in Table S2. Homozygous R462Q variant of RNASEL is represented in approximately 13% of the human population (S6, S7).

Flow cytometry for detection of antiviral antibodies in CFS plasma. The murine cell lines BaF3ER and BaF3ER-SFFV Env (S8) were grown in 2 units/ml of Epo in RPMI 1640 plus 7% FCS. 500,000 cells per sample in log phase were used as targets for direct staining. Cell lines were first washed in wash buffer (2% FBS, 0.02% Na Azide, PBS) and resuspended in 200 µL of BSA staining buffer (BD PharMingen, San Jose, CA). Patient plasma was thawed rapidly and used at 20 µL or 2 µL per tube (1:10 and 1:100 respectively) and incubated at 4^{o}C or on ice for 30 minutes. Cells were then washed with 0.5mL of wash buffer. Tubes were centrifuged at 800 rpm for 5 minutes, the supernatant was removed and tubes blotted on a towel. Next, 100 µL of the following working solution was added: 5 µL human A/B sera, 1 µL biotin labeled anti-human IgG (for human plasma) or biotin-labeled anti-rat IgG (for SFFV Env mAb)(Ebioscience, San Diego, CA), 1 µL of strep/avidin phycoerythrin (PE), 94 µL cold staining buffer. Samples were then incubated at 4^{o}C for 20 minutes, washed with 0.5 mL of wash buffer, and spun at 800 rpm for 5 minutes before being analyzed by flow cytometry. For the competition experiments, 100 µL of cold staining buffer and 10 µL of human plasma were added to each tube prior to addition of either anti-SFFV Env mAb (7C10) or Y3 myeloma supernatant (control). Samples were incubated at 4^{o}C or on ice for 20 minutes, washed with 0.5 mL of wash buffer and spun at 800 rpm for 5 minutes before being analyzed by flow cytometry.

Legends:

Figure S1. Gag sequences of XMRV in CFS patients. Partial sequences (nt 649-1017) from CFS XMRV strains WPI-1130, WPI-1138 and WPI-1169 in comparison to XMRV strains VP35, VP42 and VP62 derived from prostate cancer patients. The yellow highlighting denotes the differences from the reference strain (VP62).

Figure S2. Phylogenetic Analysis of XMRV in CFS patients. Neighbor-joining analysis of CFS XMRV strains WPI-1104, WPI-1106 and WPI-1178 with previously identified XMRVs and the nonecotropic MLVs xenotropic (Xmv), polytropic (Pmv) and modified polytropic (Mmpv) (S5). Ecotropic MLVs FLV and MoMLV were included to root the tree as outgroups in the phylogenetic reconstruction. Bootstrap supports of >70% are shown next to branch nodes. The scale measures evolutionary distance in substitutions per nucleotide. Subgroup designations are marked with arrows. XMRVs (WPI and VPs) form a distinct clade clustering together and separately from the xenotropic (Xmv) proviruses (shown in red).

Figure S3. Detection of cloned XMRV-VP62 using a rat mAb to SFFV Env and a goat antiserum to mouse NZB xenotropic MLV. **A**. Lysates were prepared from XMRV-VP62-infected Raji (lane1), LNCaP (lane 2) or Sup-T1 (lane 3). Positive

controls used were HCD-57 cells, a mouse erythroleukemia cell line expressing polytropic MLV gp70 Env (lane 4), and HCD-57 cells infected with SFFV, which also express SFFV gp55 Env (lane 5). WB analysis was carried out using rat anti-SFFV Env mAb 7C10. Molecular weight markers in kD are shown on the left. **B.** Lysates were prepared from XMRV-VP62-infected Raji (lane 1), LNCaP (lane 2) or Sup-T1 (lane 3). Lysates from SFFV-infected mouse HCD-57 cells (lane 4) and from uninfected Raji, LNCaP and Sup-T1 are shown in lanes 5-7, respectively. WB was carried out using goat antiserum to mouse NZB xenotropic MLV. Molecular weight markers in kD are shown on the left.

Figure S4. Expression of XMRV proteins in PBMC from CFS patients. **A.** Activated B cells from CFS patient WPI-1125, activated T cells from CFS patient WPI-1105 or normal activatedT cells were incubated with goat antisera (black area) against Rauscher MLV gp70 Env (top), p30 Gag (middle) and p10 Gag (bottom) and analyzed by IFC. Preimmune goat serum (light area) was used as a control. **B.** A B cell line from a CFS patient was incubated with rat anti-SFFV Env mAb (right panel) or control myeloma supernatant (left panel) and then analyzed by IFC. **C.** Lysates were prepared from B cells (lane 1) or T cells (lanes 2 and 3) from CFS patients that had been grown for 42 days on CD40L or IL-2 respectively were analyzed by WB using rat anti-SFFV Env mAb (top panel) or goat anti-NZB xenotropic MLV serum (bottom panel). Lane 4: normal T cells; Lane 5: mouse HCD-57 cells; Lane 7: SFFV-infected HCD-57 cells. Molecular weight markers in kD are shown on the left.

Figure S5: Infectious XMRV in CFS patients' PBMC and plasma**. A**. The indicated T-cell cultures from CFS patients were co-cultured with LNCaP as described in the Methods. XMRV p30 Gag expression was detected in the LNCaP cells using a rat anti-MLV p30 Gag mAb and IFC. Bottom panel: LNCaP co-cultured with normal T cells. B. Plasma from the indicated CFS patients was co-cultured with LNCaP. At the second passage, XMRV p30 Gag expression in the LNCaP cells was detected by flow cytometry using a rat anti-MLV p30 Gag monoclonal Ab. Co-culture with plasma from a normal healthy donor is shown in the bottom panel.

Figure S6: Presence of antibodies in CFS plasma that recognize the cell surface of SFFV Env expressing BAF3ER cells. **A.** Plasma from CFS patients or normal healthy controls was diluted 1:10, reacted with BaF3-ER or BaF3ER-SFFV Env cells and analyzed by IFC. Shown is the difference in mean fluorescence intensity (MFI) between CFS and control plasma direct binding to BaF3ER-SFFV Env cells versus BaF3ER (control) cells. **B.** Competition experiment, carried out as described in the Methods, showing that plasma from a CFS patient can block binding of a rat anti-SFFV Env mAb to BaF3ER-SFFV Env cells. Left panel: CFS plasma diluted 1:10 (white area) eliminates most of the anti-SFFV Env binding (striped area) and overlaps with the negative control (black area). Right panel: CFS plasma diluted 1:100 (white area) eliminates less

of the anti-SFFV Env binding (striped area) and overlaps much more with the positive than the negative control (black area).

Supporting References

S1. Fukuda, K., S. E. Straus, et al. *Ann, Intern. Med.,* **121,** 953(1994).

S2. E. DeFreitas *et al.*, *Proc Natl Acad Sci U S A* **88**, 2922 (1991).

S3. JD Thompson *et al*., *Nucleic Acids Res* **25,**4876 (1997).

S4. K. Tamura *et al., Molecular Biology and Evolution* **24,**1596 (2007).

S5. P. Jern, J.P. Stoye, J.M. Coffin, *PLOS Genetics* **3,** e183 (2007).

S6. A. Rokman *et al.*, *Am J Hum Genet* **70**, 1299 (May, 2002).

S7. L. Wang *et al.*, *Am J Hum Genet* **71**, 116 (2002).

S8. K. Nishigaki *et al*., *J Virol* **75,** 7893 (2001)

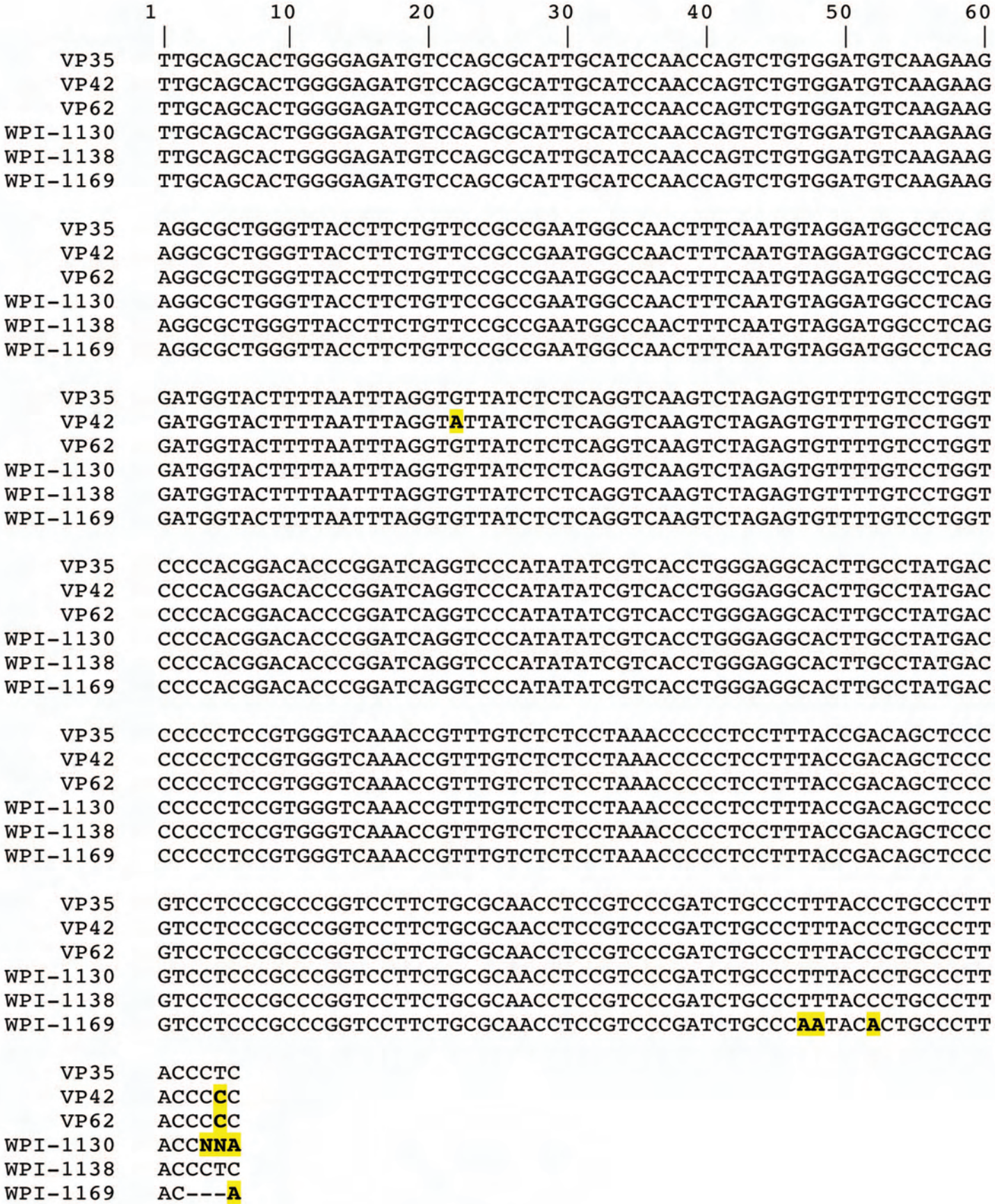
1 10 20 30 40 50 60
VP35 TTGCAGCACTGGGGAGATGTCCAGCGCATTGCATCCAACCAGTCTGTGGATGTCAAGAAG
VP42 TTGCAGCACTGGGGAGATGTCCAGCGCATTGCATCCAACCAGTCTGTGGATGTCAAGAAG
VP62 TTGCAGCACTGGGGAGATGTCCAGCGCATTGCATCCAACCAGTCTGTGGATGTCAAGAAG
WPI-1130 TTGCAGCACTGGGGAGATGTCCAGCGCATTGCATCCAACCAGTCTGTGGATGTCAAGAAG
WPI-1138 TTGCAGCACTGGGGAGATGTCCAGCGCATTGCATCCAACCAGTCTGTGGATGTCAAGAAG
WPI-1169 TTGCAGCACTGGGGAGATGTCCAGCGCATTGCATCCAACCAGTCTGTGGATGTCAAGAAG
VP35 AGGCGCTGGGTTACCTTCTGTTCCGCCGAATGGCCAACTTTCAATGTAGGATGGCCTCAG
VP42 AGGCGCTGGGTTACCTTCTGTTCCGCCGAATGGCCAACTTTCAATGTAGGATGGCCTCAG
VP62 AGGCGCTGGGTTACCTTCTGTTCCGCCGAATGGCCAACTTTCAATGTAGGATGGCCTCAG
WPI-1130 AGGCGCTGGGTTACCTTCTGTTCCGCCGAATGGCCAACTTTCAATGTAGGATGGCCTCAG
WPI-1138 AGGCGCTGGGTTACCTTCTGTTCCGCCGAATGGCCAACTTTCAATGTAGGATGGCCTCAG
WPI-1169 AGGCGCTGGGTTACCTTCTGTTCCGCCGAATGGCCAACTTTCAATGTAGGATGGCCTCAG
VP35 GATGGTACTTTTAATTTAGGTGTTATCTCTCAGGTCAAGTCTAGAGTGTTTTGTCCTGGT
VP42 GATGGTACTTTTAATTTAGGTATTATCTCTCAGGTCAAGTCTAGAGTGTTTTGTCCTGGT
VP62 GATGGTACTTTTAATTTAGGTGTTATCTCTCAGGTCAAGTCTAGAGTGTTTTGTCCTGGT
WPI-1130 GATGGTACTTTTAATTTAGGTGTTATCTCTCAGGTCAAGTCTAGAGTGTTTTGTCCTGGT
WPI-1138 GATGGTACTTTTAATTTAGGTGTTATCTCTCAGGTCAAGTCTAGAGTGTTTTGTCCTGGT
WPI-1169 GATGGTACTTTTAATTTAGGTGTTATCTCTCAGGTCAAGTCTAGAGTGTTTTGTCCTGGT
VP35 CCCCACGGACACCCGGATCAGGTCCCATATATCGTCACCTGGGAGGCACTTGCCTATGAC
VP42 CCCCACGGACACCCGGATCAGGTCCCATATATCGTCACCTGGGAGGCACTTGCCTATGAC
VP62 CCCCACGGACACCCGGATCAGGTCCCATATATCGTCACCTGGGAGGCACTTGCCTATGAC
WPI-1130 CCCCACGGACACCCGGATCAGGTCCCATATATCGTCACCTGGGAGGCACTTGCCTATGAC
WPI-1138 CCCCACGGACACCCGGATCAGGTCCCATATATCGTCACCTGGGAGGCACTTGCCTATGAC
WPI-1169 CCCCACGGACACCCGGATCAGGTCCCATATATCGTCACCTGGGAGGCACTTGCCTATGAC
VP35 CCCCCTCCGTGGGTCAAACCGTTTGTCTCTCCTAAACCCCCTCCTTTACCGACAGCTCCC
VP42 CCCCCTCCGTGGGTCAAACCGTTTGTCTCTCCTAAACCCCCTCCTTTACCGACAGCTCCC
VP62 CCCCCTCCGTGGGTCAAACCGTTTGTCTCTCCTAAACCCCCTCCTTTACCGACAGCTCCC
WPI-1130 CCCCCTCCGTGGGTCAAACCGTTTGTCTCTCCTAAACCCCCTCCTTTACCGACAGCTCCC
WPI-1138 CCCCCTCCGTGGGTCAAACCGTTTGTCTCTCCTAAACCCCCTCCTTTACCGACAGCTCCC
WPI-1169 CCCCCTCCGTGGGTCAAACCGTTTGTCTCTCCTAAACCCCCTCCTTTACCGACAGCTCCC
VP35 GTCCTCCCGCCCGGTCCTTCTGCGCAACCTCCGTCCCGATCTGCCCTTTACCCTGCCCTT
VP42 GTCCTCCCGCCCGGTCCTTCTGCGCAACCTCCGTCCCGATCTGCCCTTTACCCTGCCCTT
VP62 GTCCTCCCGCCCGGTCCTTCTGCGCAACCTCCGTCCCGATCTGCCCTTTACCCTGCCCTT
WPI-1130 GTCCTCCCGCCCGGTCCTTCTGCGCAACCTCCGTCCCGATCTGCCCTTTACCCTGCCCTT
WPI-1138 GTCCTCCCGCCCGGTCCTTCTGCGCAACCTCCGTCCCGATCTGCCCTTTACCCTGCCCTT
WPI-1169 GTCCTCCCGCCCGGTCCTTCTGCGCAACCTCCGTCCCGATCTGCCCAATACACTGCCCTT
VP35 ACCCTC
VP42 ACCCCC
VP62 ACCCCC
WPI-1130 ACCNNA
WPI-1138 ACCCTC
WPI-1169 AC---A

Figure S1

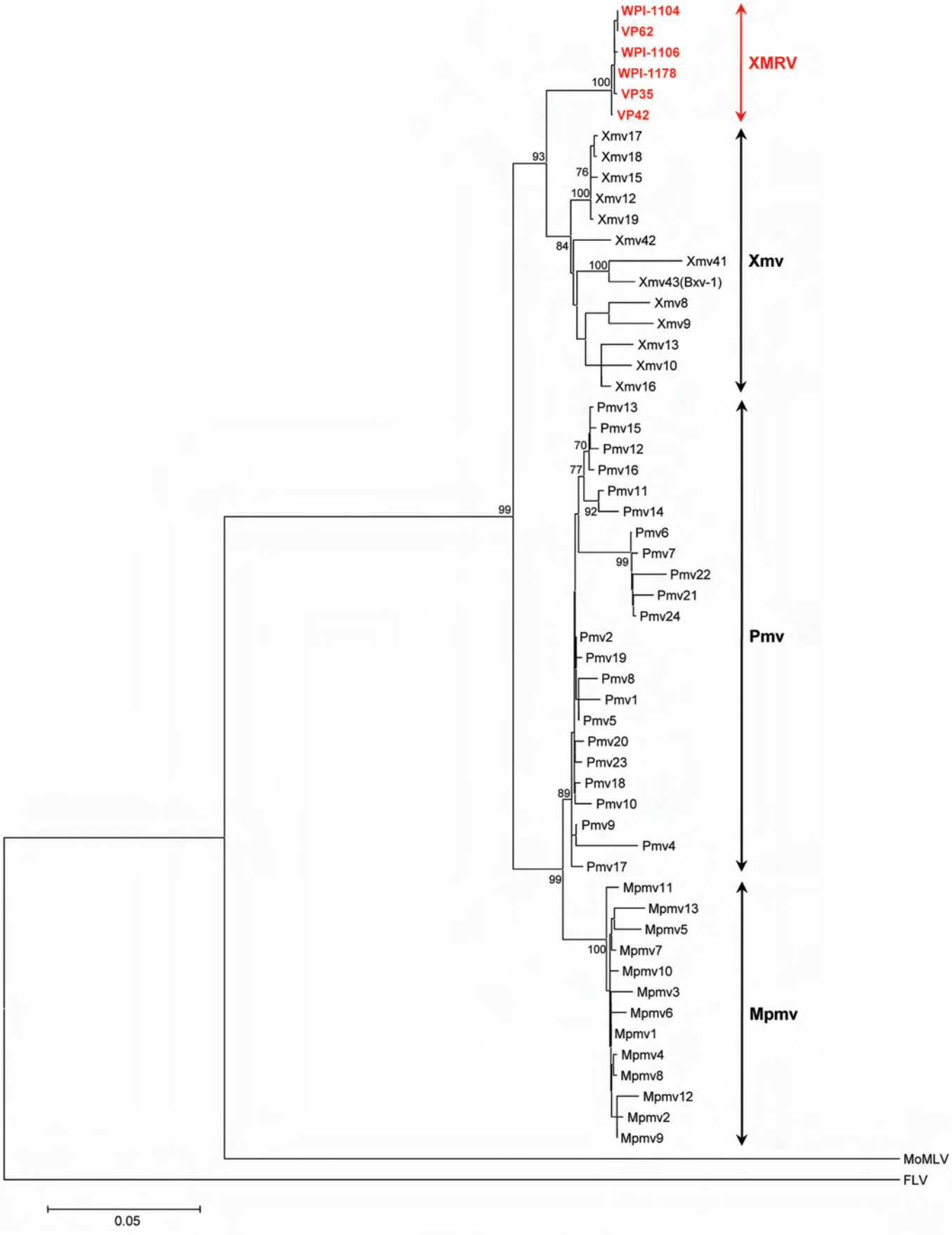
WPI-1104
VP62
WPI-1106
WPI-1178
VP35
VP42
XMRV
100
Xmv17
Xmv18
93
Xmv15
76
Xmv12
100
Xmv19
Xmv42
84
Xmv41
100
Xmv43(Bxv-1)
Xmv8
Xmv9
Xmv13
Xmv10
Xmv16
Xmv
Pmv13
Pmv15
70
Pmv12
77
Pmv16
Pmv11
92
Pmv14
99
Pmv6
Pmv7
99
Pmv22
Pmv21
Pmv24
Pmv2
Pmv19
Pmv8
Pmv1
Pmv5
Pmv20
Pmv23
Pmv18
89
Pmv10
Pmv9
Pmv4
Pmv17
Pmv
99
Mpmv11
Mpmv13
Mpmv5
100
Mpmv7
Mpmv10
Mpmv3
Mpmv6
Mpmv1
Mpmv4
Mpmv8
Mpmv12
Mpmv2
Mpmv9
Mpmv
MoMLV
FLV
0.05

Figure S2

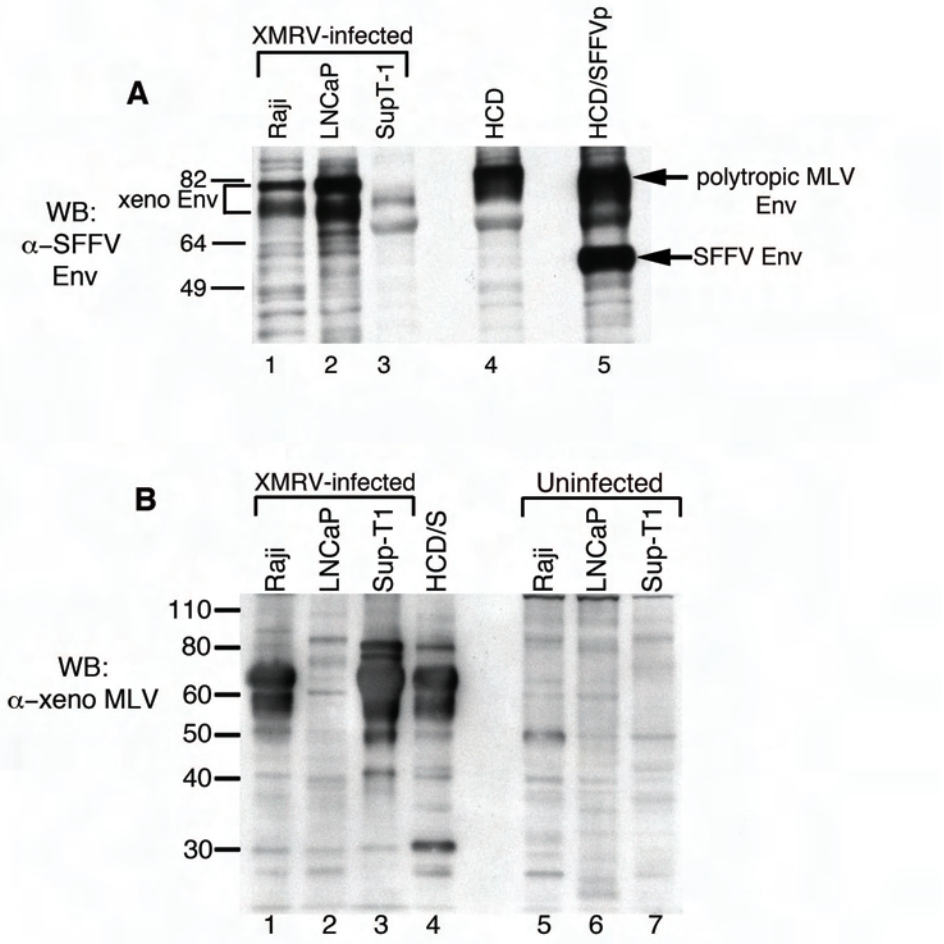
A
XMRV-infected
Raji
LNCaP
SupT-1
HCD
HCD/SFFVp
WB:
α–SFFV
Env
82
xeno Env
64
49
polytropic MLV
Env
SFFV Env
1
2
3
4
5
B
XMRV-infected
Uninfected
Raji
LNCaP
Sup-T1
HCD/S
Raji
LNCaP
Sup-T1
WB:
α–xeno MLV
110
80
60
50
40
30
1
2
3
4
5
6
7

Figure S3

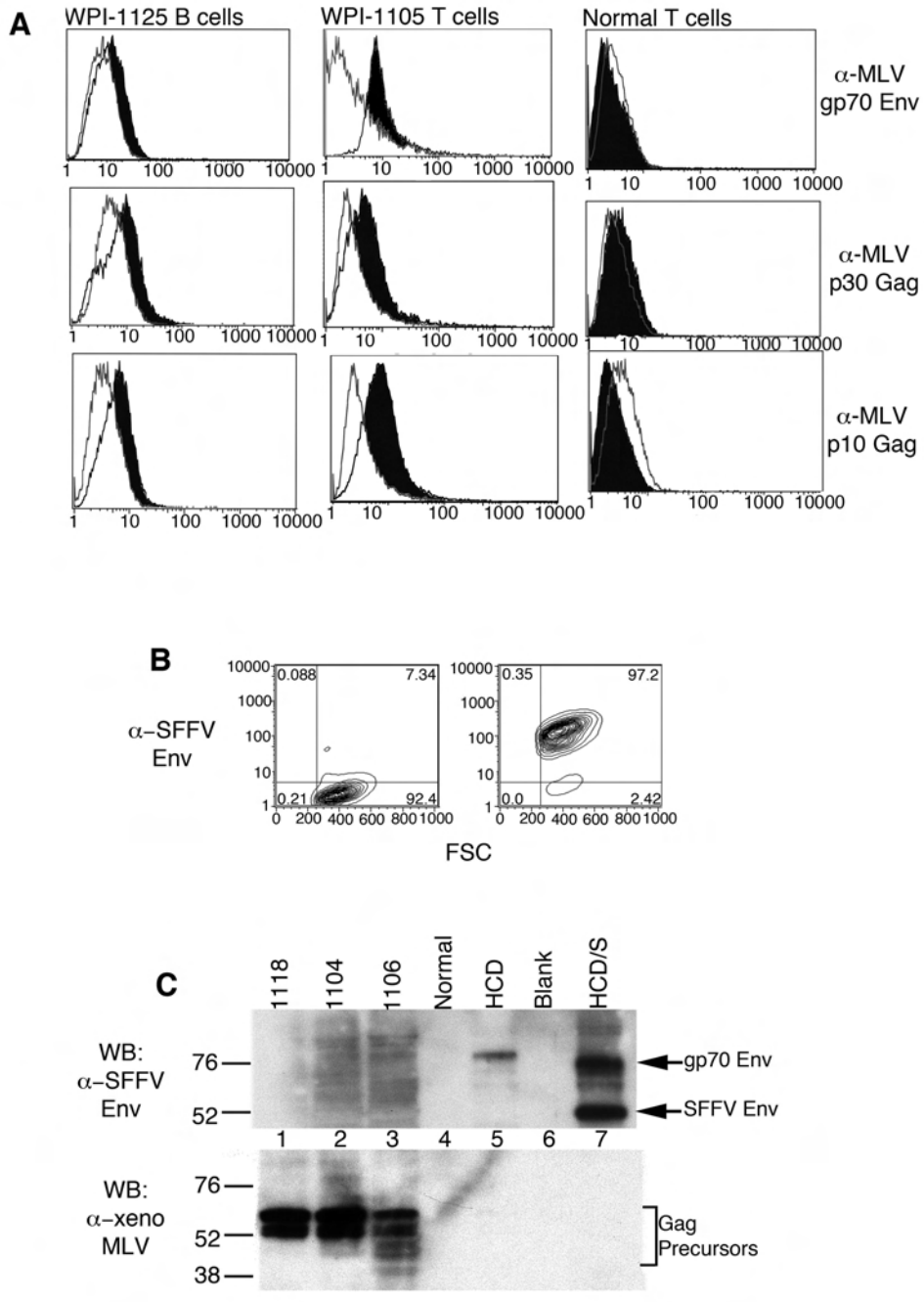
A
WPI-1125 B cells
WPI-1105 T cells
Normal T cells
α-MLV gp70 Env
α-MLV p30 Gag
α-MLV p10 Gag
B
α–SFFV Env
0.088
7.34
0.21
92.4
0.35
97.2
0.0
2.42
FSC
C
1118
1104
1106
Normal
HCD
Blank
HCD/S
WB: α–SFFV Env
76
52
gp70 Env
SFFV Env
1 2 3 4 5 6 7
WB: α–xeno MLV
76
52
38
Gag Precursors

Figure S4

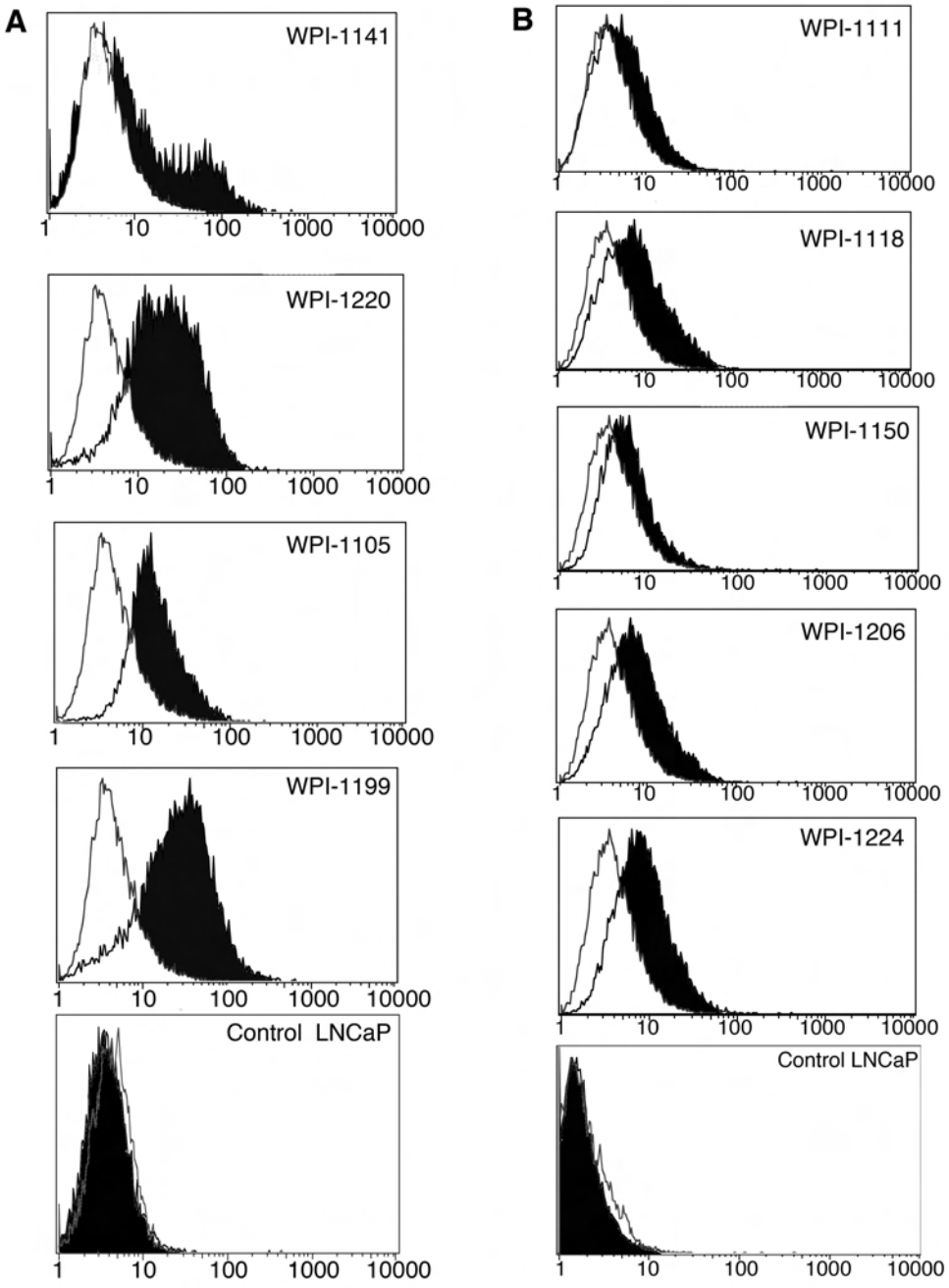
A
WPI-1141
WPI-1220
WPI-1105
WPI-1199
Control LNCaP
B
WPI-1111
WPI-1118
WPI-1150
WPI-1206
WPI-1224
Control LNCaP
1
10
100
1000
10000

Figure S5

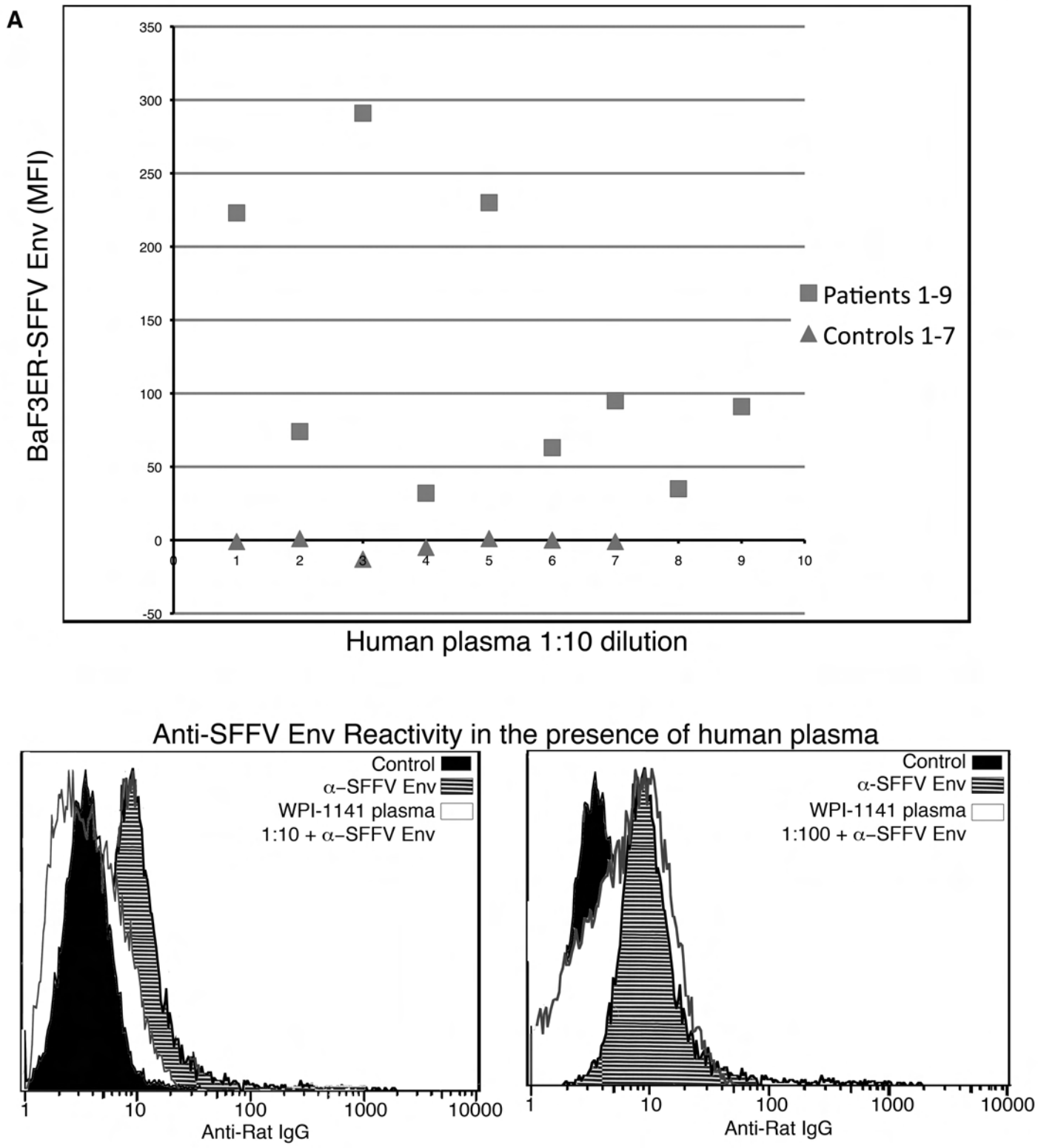
A
BaF3ER-SFFV Env (MFI)
350
300
250
200
150
100
50
0
-50
0
1
2
3
4
5
6
7
8
9
10
Patients 1-9
Controls 1-7
Human plasma 1:10 dilution
B
Anti-SFFV Env Reactivity in the presence of human plasma
Control
α–SFFV Env
WPI-1141 plasma
1:10 + α–SFFV Env
1
10
100
1000
10000
Anti-Rat IgG
Control
α-SFFV Env
WPI-1141 plasma
1:100 + α–SFFV Env
1
10
100
1000
10000
Anti-Rat IgG

Figure S6

Table S1. Comparison of Nucleotide Sequences of XMRV Strains from Prostate Cancer and Chronic Fatigue Syndrome Patients to XMRV VP62*						
	Prostate Cancer Cases			Chronic Fatigue Syndrome Cases		
nt (number)	VP 62 (4-8174 nt)	VP 42 (1-8186 nt)	VP 35 (1-8186 nt)	WPI-1106 (4-8147 nt)	WPI-1178 (4-8147 nt)	WPI-1104 (4-1152; 5923-8147 nt)
375			A			
450			C			
790		A				
1013			T			
1477			G			
1565		G				
1824		G	G			
2413				A		
2416						
2559			A			
2602			A			
2622		G				
4159		G				
4229		C deletion				
4236		G insertion				
4883				T		
4985				A		
5083			T			
5087			A			
5313						G
5823					C	
5830				G		
6373					G	
6651		A				
7064			G			
7357			A			
7437				G		
7451				G	G	G
7456		G	G		G	
7692					T insertion	
7777					G insertion	
7782		G insertion	G insertion			

*Accession numbers: VP62, EF185282; VP35, DQ241301; VP42, DQ241302

Table S1

Relationship between RNaseL variant genotype and XMRV expression in CFS patients

Genotype	***Population***		***XMRV Results***	
R462Q variant	**Patients**	**Controls**	**Negative**	**Positive**
AA	16	13	3	4
AG	66	36	18	26
GG	74	39	27	33
Total	**156**	**88**	**48**	**63**
X^2	0.10	0.87	0.11	
P value	0.95	0.65	0.74	

Table S2